

Microscopic and coarse-grained correlation functions in concentrated dendrimer solutions[‡]

I O Götze and C N Likos

Institut für Theoretische Physik II, Heinrich-Heine-Universität Düsseldorf,
Universitätsstraße 1, D-40225 Düsseldorf, Germany

Abstract. We employ monomer-resolved computer simulations of model dendrimer molecules, to examine the significance of many-body effects in concentrated solutions of the same. In particular, we measure the radial distribution functions and the scattering functions between the centres of mass of the dissolved dendrimers at various concentrations, reaching values that slightly exceed the overlap density of the macromolecules. We analyse the role played by many-body effective interactions by comparing the structural data to those obtained by applying exclusively the previously obtained two-body effective interactions between the dendrimers [Götze I O, Harreis H M and Likos C N 2004 *J. Chem. Phys.* **120** 7761]. We find that the effects of the many-body forces are small in general and they become weaker as the dendrimer flexibility increases. Moreover, we test the validity of the oft-used factorisation approximation to the total scattering intensity into a product of the form- and the scattering factors, finding a breakdown of this factorisation at high concentrations.

1. Introduction

Soft matter systems are characterised by the simultaneous existence of two intrinsic structural length scales: the omnipresent atomic or *microscopic* scale that is associated with the solvent molecules and the monomers of the dissolved polymers (if any) and the *mesoscopic* scale that characterises the dissolved macromolecular aggregates as a whole. Depending on the physical system under consideration, the latter typically covers the range between several nanometers and micrometers, spanning thereby three orders of magnitude. The former is rather located in the domain of a few Ångström. In attempting to bridge the scales all the way from the microscopic to the macroscopic ones, it has been proven very useful to eliminate the atomic degrees of freedom from view, by performing a statistical-mechanical trace over their degrees of freedom and constructing thereby an *effective Hamiltonian* that involves the mesoscopic degrees of freedom only [1]. Although the effective Hamiltonian \mathcal{H}_{eff} greatly facilitates the transition to the macroscopic scales, both its construction and its interpretation have to be treated with care: indeed, the effective potential energy function that involves the

[‡] This paper is dedicated to Professor Lothar Schäfer on the occasion of his 60th birthday.

mesoscopic degrees of freedom which appear in \mathcal{H}_{eff} are not true interaction potentials in the sense of Hamiltonian Mechanics but rather a constrained free energy which arises by the thermodynamic trace of the microscopic ones.

There is a number of subtleties associated with the effective potential energy function that have to be taken into account when a coarse-grained statistical mechanical treatment of a soft matter system is employed. Two of them are particularly relevant in the context of calculating thermodynamic quantities and tracing out phase diagrams. First, the potential energy cannot, in general, be written as a sum of pair interactions:§ the process of eliminating the microscopic degrees of freedom inadvertently generates higher-order, many-body potentials [2, 3, 4]. Truncating the effective potential energy function at the pair-level constitutes the *pair potential approximation*, whose validity is not *a priori* guaranteed and has to be explicitly checked. And secondly, that the contributions to the potential energy are in general state-dependent, the most prominent example of the latter being the Debye-Hückel effective pair potential that has been extensively employed to model charge-stabilised colloidal suspensions under certain physical conditions [5]. Sometimes the state-dependence of an effective pair potential hides precisely the effect of many-body forces and then particular care has to be taken in the ways in which the pair potential is employed, so as to avoid blatant thermodynamic inconsistencies [6, 7, 8, 9].

Many-body potentials are already encountered in the realm of atomic systems, the Axilrod-Teller interaction [10] being a characteristic example that has been shown to be relevant for the description of high-precision measurements of the structure factor of rare gases [11]. A formal decomposition of the effective potential energy function between the particles of one kind in a binary mixture in which the particles of the other kind are traced out has been given in Refs. [3] and [4]. Unfortunately, the treatment there applies only to mixtures for which the number densities of the two components can be varied at will, e.g., colloid-polymer or hard-sphere mixtures. It is not applicable to two broad categories of soft matter systems, namely charged mixtures and solutions of polymers of arbitrary architecture. In the former case, the number densities of the two components are constrained by the electroneutrality condition. In the latter, where one specific monomer [12, 13] or the centre of mass of the molecule [14, 15, 16, 17, 18] are chosen as effective, mesoscopic coordinates, the total number of monomers and the number of effective particles are coupled to each other through the constraint of keeping the number of monomers per macromolecule fixed.

In charge-stabilised colloidal suspensions, three-body forces are generated by nonlinear counterion screening. Their effects have been examined by density functional theory and simulations [19] as well as by numerical solution of the nonlinear-Poisson Boltzmann equation [20, 21]. It has been found that the three-body forces in this case

§ An important exception, however, is the depletion attraction in colloid-polymer mixtures described by the idealised Asakura-Oosawa model. In this case, all n -th order polymer-mediated effective interactions between colloids vanish identically for $n \geq 3$ if the polymer-to-colloid size ratio does not exceed $2\sqrt{3}/3 - 1$. See Ref. [2] for details.

are *attractive* [19, 20, 21], a result confirmed by direct experimental measurements using optical tweezers [20, 21]. As far as polymeric systems are concerned, the triplet forces in star polymer solutions have been analysed by theory and simulations in Ref. [22], where it was found that they play a minor role for concentrations vastly exceeding the overlap density. For linear chains, on the other hand, the many-body forces appear to have a more pronounced effect, as witnessed by the considerable state-dependence of the effective pair potential that reproduces the correlation functions of concentrated polymer solutions [17, 18]. The general functional form of the centre-of-mass effective interaction between polymer chains was found to preserve its Gaussian form, its strength and range being nevertheless modified within a range of $\sim 10\%$ of their original values, due to many-body effects [17, 18].

Another polymeric system that serves as a prototype for a tunable colloidal system that displays a Gaussian, soft effective pair interaction is that of a solution of dendritic macromolecules, or dendrimers for simplicity [23]. It has been recently shown that a Gaussian effective pair potential can describe extremely well the scattering intensities obtained experimentally from concentrated dendrimer solutions [24, 25]. The Gaussian pair interaction has also been explicitly measured in recent computer simulations that employed two different coarse-grained models for the microscopic, monomer-monomer interactions [26]. Nevertheless, in the approach of Ref. [26] only *two* dendritic molecules were simulated, hence no information about many-body forces was gained. In the present work, we address the issue of the magnitude and importance of many-body effective interaction potentials in concentrated dendrimer solutions. We do not attempt to derive an explicit decomposition of the potential energy function into n -body terms, $n = 2, 3, 4, \dots$; this would require separate simulations of just n dendrimers. Instead, we explicitly simulate a large number of interacting dendrimers at the microscopic level simultaneously. We measure thereby the pair correlation functions in the concentrated system directly and we compare the result with the one obtained by simulating the *same* number of dendrimers as effective entities interacting exclusively by means of pair potentials. The discrepancies in the results from the two approaches for the correlation functions yield then information regarding the importance of the many-body forces *of all orders*. We find that the many-body effects are of minor importance, especially for flexible dendrimers.

The rest of the paper is organised as follows. In section 2 we present our model and the simulation details. In section 3 we present our results for the correlation functions derived by the two approaches mentioned above and we discuss the magnitude and origin of their discrepancies. In section 4 we turn our attention to the issue of the interpretation of the total scattering intensities from concentrated dendrimer solutions, and in particular to the question of the validity of the so-called factorisation approximation of the latter as the product of the form- and the structure factor, discussing the limits of applicability of such an approach. Finally, in section 5 we summarise and conclude.

2. The model and simulation details

In this work, we focus exclusively on dendrimers of the fourth generation (G4). We model the macromolecules at the monomer-level using a simplified model that pictures every monomer as a hard sphere of diameter σ . The bonding between the connected monomers is modeled by flexible threads of maximum extension $\sigma(1 + \delta)$. In detail, the potential between *disconnected* monomers is given by

$$V_{\text{HS}}(r) = \begin{cases} \infty & \text{for } r/\sigma < 1 \\ 0 & \text{for } r/\sigma > 1 \end{cases} \quad (1)$$

whereas *bonded* monomers interact via the potential

$$V_{\text{bond}}(r) = \begin{cases} \infty & \text{for } r/\sigma < 1 \\ 0 & \text{for } 1 < r/\sigma < 1 + \delta \\ \infty & \text{for } r/\sigma > 1 + \delta \end{cases} \quad (2)$$

The quantity $\delta > 0$ serves as a control parameter of the dendrimer conformations, with small δ -values resulting into stiff dendrimers and large values into loose structures. This bead-thread model was originally introduced by Sheng *et al.* [27], who kept a fixed value $\delta = 0.4$ and examined the scaling of the radius of gyration of the dendrimers as a function of generation number and spacer length. The same model has been employed in a previous work by us, in order to systematically examine the evolution of the dendrimers' conformational properties with the generation number G [28]. By comparing the results for various values of the parameter δ and by performing a further comparison with results from a different model, we have shown that the conformational properties of single dendrimers are insensitive with respect to the details of the microscopic model. Moreover, this very simple, coarse-grained model reproduces the experimental scattering data for isolated dendrimers very well [28]. As we are only interested in static properties, we also allow 'ghost chains', i.e., crossing of bonds occurring for $\delta \geq \sqrt{2} - 1 \approx 0.414$ are possible. Monte Carlo simulations of this model are very fast, as there is no need to calculate energies; one only needs to check for overlaps, and additionally whether the conditions of the maximal bond extension are fulfilled. If one of these conditions is violated, the trial move is rejected in any case, so the search for further overlaps can be aborted. Furthermore, due to the very short range of the hard sphere interaction, neighbour lists are very effective.

The effective *pair* interaction potential between the centres of mass of two G4-dendrimers has been determined with the help of configuration-biased Monte Carlo simulations of this model in Ref. [26]. The strength of the interaction between dendrimers can be tuned by varying the number of generations or the parameter δ . Denoting by r the centre of mass separation, the δ -dependent effective pair potential $V_{\text{eff}}^{(2)}(r; \delta)$ has been found to have a Gaussian form with small, additional corrections. In particular, it can be fitted by the function:

$$\beta V_{\text{eff}}^{(2)}(r; \delta) = \epsilon_0 \exp\left(-\frac{r^2}{\gamma_0}\right) + \epsilon_1 \exp\left[-\frac{(r - r_1)^2}{\gamma_1}\right] - \epsilon_2 \exp\left[-\frac{(r - r_2)^2}{\gamma_2}\right], \quad (3)$$

Table 1. The numerical values of the fit parameters of the effective pair potential between the centres of mass of two G4-dendrimers appearing in Eq. (3) for two different values of δ . At the last column the gyration radius $R_{g,\infty}$ at infinite dilution is also shown.

δ	ϵ_0	γ_0/σ^2	ϵ_1	γ_1/σ^2	r_1/σ	ϵ_2	γ_2/σ^2	r_2/σ	$R_{g,\infty}/\sigma$
0.1	55.75	9.75	5.0	0.9	2.5	0.1	1.5	7.2	2.665
2.0	11.35	33.0	0.8	10.0	3.7	0.0	—	—	4.939

where $\beta = (k_B T)^{-1}$ with Boltzmann's constant k_B and the absolute temperature T ; the numerical values of the various fit parameters, depending on the choice of δ , are given in Table 1. Note that the precise values of the fit parameters are slightly different than those given in Ref. [26], since there we employed a more constrained fit by setting $\gamma_0 = 4R_{g,\infty}^2/3$, with the radius of gyration $R_{g,\infty}$ of the dendrimers at infinite dilution, and $\epsilon_2 = 0$. The gyration radius is also shown at the last column of Table 1. Here, we considered G4-dendrimers with two different values, $\delta = 0.1$ and $\delta = 2.0$, representing the two extreme cases studied in Ref. [26].

Let $\rho = N/\Omega$ be the number density of a sample containing N dendrimers enclosed in the volume Ω . The definition of the overlap density ρ_* of a dendrimer solution requires some care, as it is not a sharply defined quantity. Previous simulation studies with this system [28] have revealed that the monomer density profiles around the dendrimer's centre of mass decay to zero at a distance $r_c \cong 1.5 R_{g,\infty}$. Motivated by this fact, we envision every dendrimer as a 'soft sphere' of radius r_c and define the overlap density through the relation:||

$$\frac{4\pi}{3}\rho_*r_c^3 = 1. \quad (4)$$

Moreover, we introduce the diameter of gyration at infinite dilution, $\tau \equiv 2R_{g,\infty}$, as the characteristic mesoscopic length scale to be used to introduce a dimensionless expression for the number density, $\rho\tau^3$. In these terms, the overlap density of Eq. (4) above is given by $\rho_*\tau^3 = 0.566$. The highest density in the simulation was $\rho_{\max}\tau^3 = 0.605$, slightly exceeding the overlap value, since $\rho_{\max} = 1.07\rho_*$.

For both values of δ , ten different concentrations were simulated, in particular at the densities $\rho/\rho_{\max} = 0.1, 0.2, \dots, 1.0$. Periodic boundary conditions were employed throughout. At all densities, systems of 500 dendrimers were simulated, whereby each dendrimer consists of $\nu = 62$ monomers, and the size of the simulation box was changed in order to modify the dendrimer number density. The minimum box length was $L_{\min} = 9.384\tau$, yielding a system with the density ρ_{\max} . The equilibration criterion for the system at hand requires some care, as there are is no internal energy in the microscopic model, since all interactions are either zero or infinity. We therefore took

|| In the literature, there are alternative definitions. For polymer chains, for instance, the definition $\frac{4\pi}{3}\rho_*R_g^3 = 1$ was used in Ref. [17].

advantage of the fact that the *effective*, pair interaction $V_{\text{eff}}^{(2)}(r; \delta)$ between the centres of mass is known and given by Eq. (3) with the parameters given in Table 1. Hence, we chose to monitor the total effective pair potential energy $U^{(2)}(N; \delta)$ given by

$$U^{(2)}(N; \delta) = \frac{1}{2} \sum_{i=1}^N \sum_{j \neq i}^N V_{\text{eff}}^{(2)}(|\mathbf{r}_i - \mathbf{r}_j|; \delta), \quad (5)$$

where $\mathbf{r}_{i,j}$ denotes the position of the i, j -th centre of mass.

Two different starting configurations were tried. In the first one, the centres of mass dendrimers possessing identical microscopic conformations were placed at the vertices of a fcc-lattice, which was achieved without violation of the excluded volume conditions. This procedure is particularly useful especially at the highest density, ρ_{max} , where a random distribution of the centres of mass will result with high probability into a forbidden state with monomer overlaps. The system was then equilibrated, monitoring $U^{(2)}(N; \delta)$ described above. In the second one, the dendrimers' centres of mass were placed in a random arrangement. Although this procedure requires a large number of failed attempts before an allowed configuration is found, especially at high densities, such configurations are possible. Once again, we monitored the total effective pair potential energy during the equilibration period, finding that it converges to the same value as the one obtained from the fcc-initial state. In this way, sufficient equilibration of the system was guaranteed. Finite-size effects were checked by selectively simulating some systems with 256 of dendrimers, in a box having a correspondingly smaller volume, so that the same density is achieved, and finding agreement between the two attempts.

For $\delta = 0.1$, $N_{\text{equil}} = 10^7$ MC steps were used to equilibrate the system, and about $N_{\text{run}} = 2 \times 10^8$ steps to gather statistics. Statistical averages were calculated every $N_{\text{meas}} = 10\,000$ MC steps. For $\delta = 2.0$, where a much larger random displacement for the monomers can be used, the equilibration phase consisted of $N_{\text{equil}} = 10^6$ steps and statistical averages were calculated every $N_{\text{meas}} = 1000$ steps over a period of $N_{\text{run}} = 2 \times 10^8$ steps. The quantities measured were monomer profiles around the centres of mass, the radial distributions functions of the latter, radii of gyration, form factors, structure factors from the centres of mass and total scattering intensities; all these quantities will be precisely defined in the sections that follow.

In Figs. 1 and 2, we show simulation snapshots of the monomer-resolved simulations for the lowest and the highest density for the thread length $\delta = 0.1$. (For clarity, in Fig. 1 we show only a section of the simulation box of the same size as in Fig. 2.) Although at Fig. 1 individual dendrimer molecules can still be resolved, since the density is much smaller than ρ_* , in Fig. 2 this is not any more possible. Here, $\rho = 1.07\rho_*$ and the whole system appears as a dense solution of monomers, in which the individual character of each macromolecule is lost. We will return to the implications of this fact in section 4.

In addition, a different kind of Monte Carlo simulations was also carried out, in which the monomers were not explicitly resolved. Instead, the dendrimers were replaced entirely by their centres of mass, which were then treated as effective, soft particles interacting exclusively by means of the pair potential of Eq. (3). Accordingly, we call

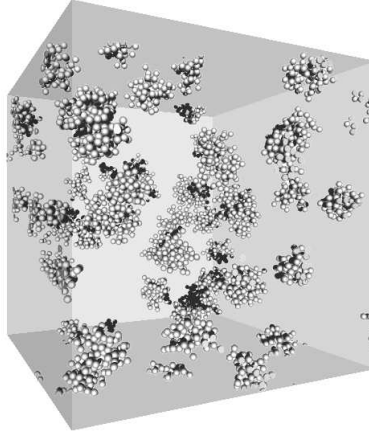


Figure 1. A snapshot from the monomer resolved-simulation of dendrimers. The monomers are rendered as spheres of diameter σ . Here, dendrimers with threads characterised through $\delta = 0.1$ at a density $\rho\tau^3 = 0.0605$ are shown. Note that only a part of the simulation box is shown, which has the same size as the full box depicted in Fig. 2.

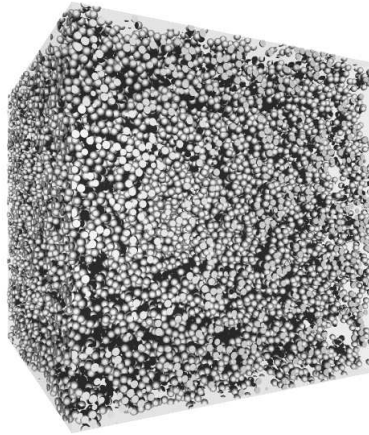


Figure 2. Same as Fig. 1 but at density $\rho\tau^3 = 0.605$. Here the complete simulation box is shown.

this approach an *effective* simulation. As all monomers have dropped out of sight in the effective approach, it is only possible to measure quantities pertaining to the centres of mass, i.e., their radial distribution functions and structure factors. Comparison of the results regarding these quantities that are obtained through the two different types of simulations yields important information by way of testing whether the pair-potential approximation is meaningful.

3. Comparison between the monomer-resolved and the effective simulations

Each dendrimer of the fourth generation consists of $\nu = 62$ monomers. Let α, β be monomer indices within a given dendrimer whereas i, j are integers describing the dendrimer molecules as whole entities. In particular, let \mathbf{r}_i stand for the position of the centre of mass of the i -th dendrimer, \mathbf{R}_α^i denote the position vector of the α -th monomer in the i -th dendrimer, and \mathbf{u}_α^i stand for the same quantity but now measured in a coordinate system centred at \mathbf{r}_i . Obviously, it holds

$$\mathbf{R}_\alpha^i = \mathbf{r}_i + \mathbf{u}_\alpha^i. \quad (6)$$

In the monomer-resolved simulation, the following quantities were measured: The radial distribution function $g(r)$ between the centres of mass, defined as

$$g(r) = \frac{1}{N} \left\langle \sum_{i=1}^N \sum_{j \neq i}^N \delta(\mathbf{r} - \mathbf{r}_{ij}) \right\rangle, \quad (7)$$

where $\langle \dots \rangle$ denotes a statistical average and $\mathbf{r}_{ij} = \mathbf{r}_i - \mathbf{r}_j$. Related to this quantity is the structure factor $S(q)$ that describes the correlations between the centres of mass in reciprocal space and it is given by

$$S(q) = \frac{1}{N} \left\langle \sum_{i=1}^N \sum_{j=1}^N \exp[-i\mathbf{q} \cdot (\mathbf{r}_i - \mathbf{r}_j)] \right\rangle. \quad (8)$$

Note that $S(q)$ and $g(r)$ are related by a Fourier transformation [29]

$$S(q) = 1 + \rho \int d^3r \exp[-i\mathbf{q} \cdot \mathbf{r}] [g(r) - 1]. \quad (9)$$

Moreover, we took advantage of the microscopic nature of the simulation to measure the dendrimers' form factor $F(q)$ at every simulated density ρ . This quantity is expressed by the relation:

$$F(q) = \frac{1}{N} \sum_{i=1}^N \frac{1}{\nu} \left\langle \sum_{\alpha=1}^{\nu} \sum_{\beta=1}^{\nu} \exp[-i\mathbf{q} \cdot (\mathbf{u}_\alpha^i - \mathbf{u}_\beta^i)] \right\rangle, \quad (10)$$

Another quantity of interest is the monomer distribution around the centre of mass, $\xi(u)$, which can again be measured at any desired overall density and is given by the expression:

$$\xi(u) = \frac{1}{N} \sum_{i=1}^N \left\langle \sum_{\alpha=1}^{\nu} \delta(\mathbf{u} - \mathbf{u}_\alpha^i) \right\rangle, \quad (11)$$

The overall size of the dendrimer is characterised by its radius of gyration R_g , which was measured in the simulation by calculating the quantity:

$$R_g = \frac{1}{N} \sum_{i=1}^N \sqrt{\frac{1}{\nu} \left\langle \sum_{\alpha=1}^{\nu} \mathbf{u}_\alpha^i \cdot \mathbf{u}_\alpha^i \right\rangle}, \quad (12)$$

In Eqs. (10) - (12) above, the summand in the sum over i is the corresponding quantity (form factor, density profile, and radius of gyration, respectively) of the i -th dendrimer.

The additional summation over i and the division by the total number of dendrimers corresponds to an additional average over *all* dendrimers. Since all macromolecules are equivalent, the expectation values are identical for every summand. Finally, we also measured the scattering function $I(q)$ of the concentrated solution, which corresponds to the coherent contribution of the total scattering intensity in a SANS experiment, under the assumption that all monomers possess the same scattering length density [30, 31, 32, 33]. This is given by the equation:

$$I(q) = \frac{1}{N\nu} \left\langle \sum_{i=1}^N \sum_{j=1}^N \sum_{\alpha=1}^{\nu} \sum_{\beta=1}^{\nu} \exp[-i\mathbf{q} \cdot (\mathbf{R}_{\alpha}^i - \mathbf{R}_{\beta}^j)] \right\rangle, \quad (13)$$

i.e., it is the total coherent scattering intensity from all monomers of the system.

In the effective picture, all information regarding the monomers' degrees of freedom is lost, hence in the effective simulation we can only measure the corresponding radial distribution function $g_{\text{eff}}(r)$ and the structure factor $S_{\text{eff}}(q)$ of the centres of mass. These are given by Eqs. (7) and (8) above but with the averages now performed with the effective Hamiltonian, i.e.,

$$g_{\text{eff}}(r) = \frac{1}{N} \left\langle \sum_{i=1}^N \sum_{j \neq i}^N \delta(\mathbf{r} - \mathbf{r}_{ij}) \right\rangle_{\mathcal{H}_{\text{eff}}}, \quad (14)$$

and

$$S_{\text{eff}}(q) = \frac{1}{N} \left\langle \sum_{i=1}^N \sum_{j=1}^N \exp[-i\mathbf{q} \cdot (\mathbf{r}_i - \mathbf{r}_j)] \right\rangle_{\mathcal{H}_{\text{eff}}}. \quad (15)$$

The effective Hamiltonian \mathcal{H}_{eff} involves the momenta \mathbf{p}_i and positions \mathbf{r}_i of the centres of mass only and contains exclusively pair interactions, i.e.,

$$\mathcal{H}_{\text{eff}} = \sum_{i=1}^N \frac{\mathbf{p}_i^2}{2m} + \frac{1}{2} \sum_{i=1}^N \sum_{j \neq i}^N V_{\text{eff}}^{(2)}(|\mathbf{r}_i - \mathbf{r}_j|; \delta), \quad (16)$$

where m is the dendrimers' mass, which is irrelevant as far as static quantities of the system are concerned. A particular property of the effective description of a complex system is that it leaves all correlation functions between the coarse-grained degrees of freedom invariant *provided* that the mapping into the effective system is *exact* [1]. In other words, if the effective Hamiltonian contains the contributions to the effective potential at *all orders*, it makes no difference whether one calculates quantities such as $g(r)$ or $S(q)$ in the original, microscopic description or in the coarse-grained one. As our effective Hamiltonian \mathcal{H}_{eff} is truncated at the pair level, the deviations between $g(r)$ and $g_{\text{eff}}(r)$ or, equivalently, between $S(q)$ and $S_{\text{eff}}(q)$ will be a measure of the importance of the neglected many-body terms in Eq. (16).

Representative results comparing between the two approaches are shown in Fig. 3, pertaining to the dendrimers with $\delta = 0.1$ and in Fig. 4, which refers to dendrimers with $\delta = 2.0$. The length scale used in this plot is the zero-density gyration radius of the dendrimers, $R_{g,\infty}$. For clarity, only the results only for three different densities obtained

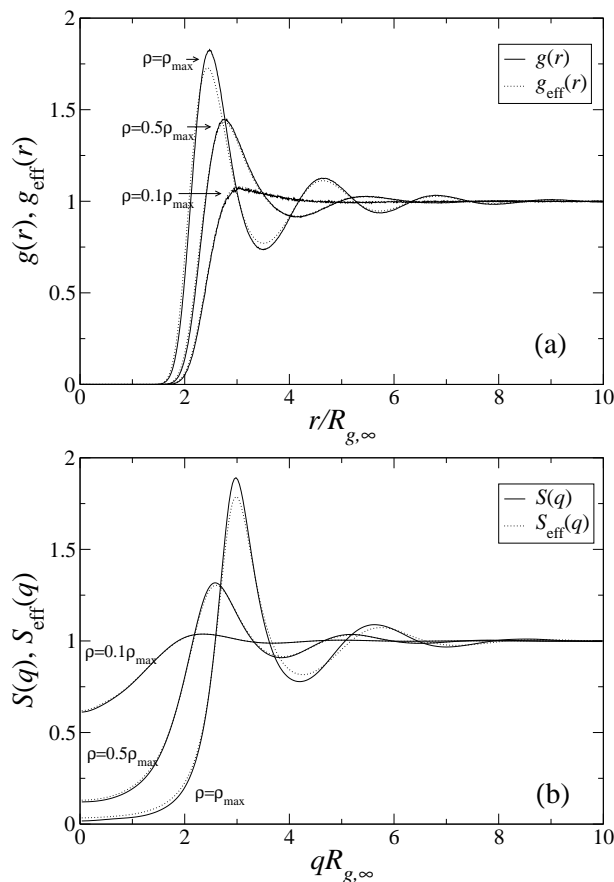


Figure 3. Comparison between the results from the monomer-resolved and the effective simulation of concentrated dendrimers with maximal thread length $\delta = 0.1$ of the bonds. The three different densities are $\rho = 0.1\rho_{\text{max}}$, $0.5\rho_{\text{max}}$ and ρ_{max} , as indicated on the plots, with $\rho_{\text{max}}\tau^3 = 0.605$. Results are shown for (a) the radial distribution function $g(r)$ and (b) the structure factor $S(q)$ of the centre of mass coordinates.

from the monomer resolved simulations are compared to those from the effective ones. At sufficiently low densities, $\rho = 0.1\rho_{\text{max}}$, the results from the two types of simulations are indistinguishable, hence the pair-potential approximation is an excellent one and many-body forces seem to play no role there; they can be thus safely ignored. Deviations between the two descriptions arise nevertheless as the overall concentration of the solution grows. Referring to Fig. 3(a), we see that for the $\delta = 0.1$ -dendrimers, which have a rather high internal monomer density, the deviations are already visible (but small) at a density $\rho = 0.5\rho_{\text{max}}$ and they become more pronounced at the highest simulated density, $\rho = \rho_{\text{max}}$. The true radial distribution function $g(r)$ between the centres of mass shows a more pronounced coordination than the effective one, $g_{\text{eff}}(r)$, and this effect is also reflected in the corresponding structure factors. The peak height of $S(q)$ is higher than the one of $S_{\text{eff}}(q)$, pointing to the fact that the zero-density pair potential underestimates somehow the strength of the repulsions between the dendrimers' centres of mass. The relative deviation between the two descriptions as far as the peak height is concerned are at the highest density about 6%. Much more drastic is the discrepancy of the $S(q \rightarrow 0)$

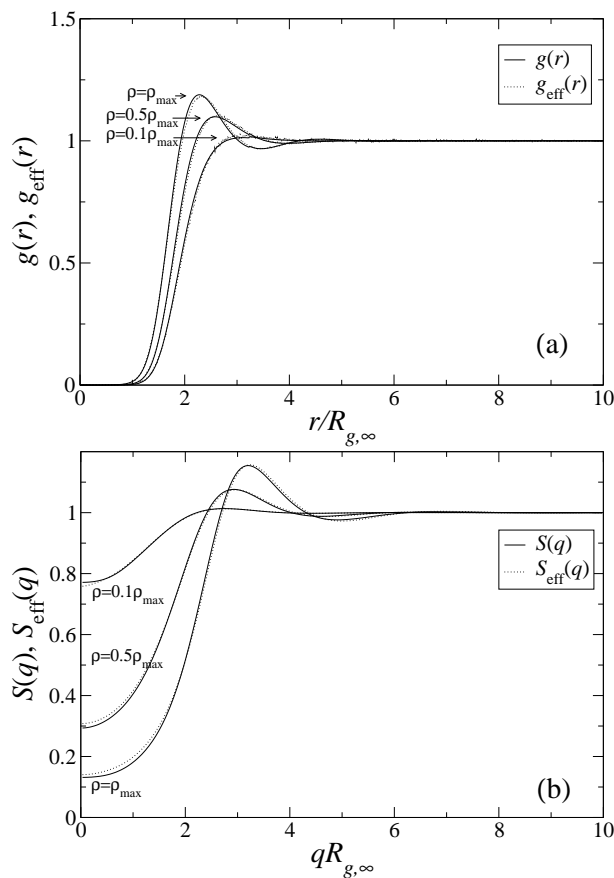


Figure 4. Same as Fig. 3 but for thread length $\delta = 2.0$.

limit, for which $S(q \rightarrow 0) = 0.018$ whereas $S_{\text{eff}}(q \rightarrow 0) = 0.033$. Given the fact that the $S(q = 0)$ -value is proportional to the osmotic isothermal compressibility of the solution, employing the effective picture can lead here to serious errors in the calculation of the thermodynamics of the system. Two integrations of the inverse compressibility are needed in order to obtain the Helmholtz free energy of the solution, hence errors at all lower densities accumulate in performing such an integration and they can lead to a serious underestimation of the free energy if the effective picture is employed.

The agreement between the microscopic and the coarse-grained approaches is a lot better for the case of the $\delta = 2.0$ -dendrimers, which possess a much lower internal monomer density than their $\delta = 0.1$ -counterparts. Indeed, as can be seen in Fig. 4(a), the radial distribution functions $g(r)$ and $g_{\text{eff}}(r)$ barely show any difference, all the way up to the maximum density ρ_{max} . Similar to the case $\delta = 0.1$, $g(r)$ shows a slightly more pronounced coordination than $g_{\text{eff}}(r)$, the difference between the two is nevertheless extremely small. The same holds for the structure factors $S(q)$ and $S_{\text{eff}}(q)$, shown in Fig. 4(b). Here, even the discrepancy in the compressibility is very small, with $S(q \rightarrow 0) = 0.132$ and $S_{\text{eff}}(q \rightarrow 0) = 0.138$ at $\rho = \rho_{\text{max}}$. For dendrimers with a higher degree of internal freedom, the pair potential approximation holds all the way up to the overlap concentration. In this respect, it is very satisfactory that it is precisely the

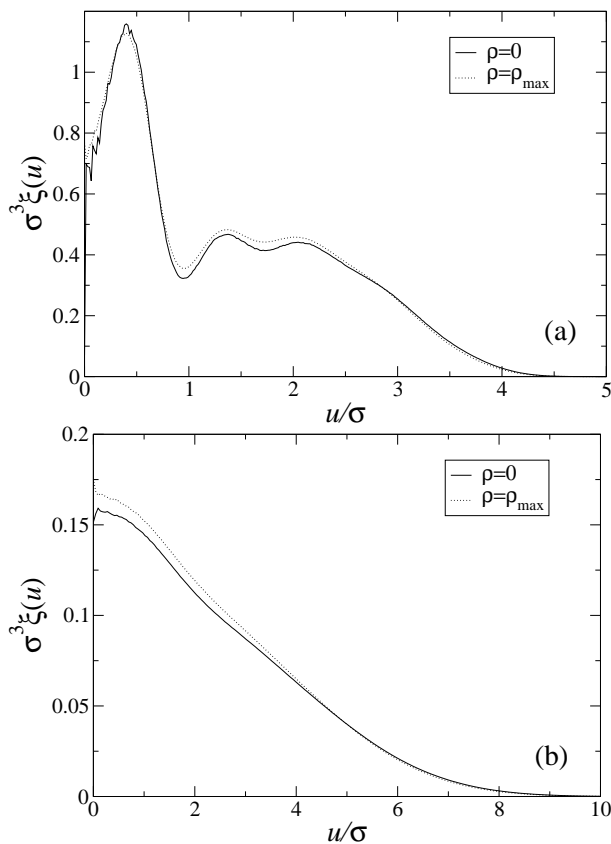


Figure 5. The radial monomer density profiles $\xi(u)$ [Eq. (11)] of the dendrimers around their centres of mass at infinite dilution ($\rho = 0$) and at the highest density $\rho = \rho_{\max} = 1.07\rho_*$, as indicated on the plots. (a) For model dendrimers with thread length $\delta = 0.1$ and (b) for $\delta = 2.0$. Note the shrinkage and growth of the profiles.

model with the value $\delta = 2.0$ that has been found to accurately describe scattering data from real dendrimers [26].

Let us now try to obtain some physical insight into the mechanisms that cause the true correlation functions to show higher ordering than the effective ones. Suppose that the reason lied in the increasing significance of three-body effective forces. Three-body potentials arise through three-dendrimer overlaps: the region of space in which three spherical objects simultaneously overlap is overcounted when one adds over the three pair interactions and it has to be subtracted anew. Given the fact that any overlap between repulsive monomers gives rise to a correspondingly repulsive interaction, together with the fact that the contribution from the triple-overlap region has to be *subtracted*, leads to the conclusion that triple forces should be *attractive*, as for the case of star polymers [22], as well as self-avoiding polymer chains [17], for which three-body forces have been measured explicitly [34]. Yet, an attractive contribution to the potential energy leads to a *reduced* effective pair repulsion. This is on the one hand intuitively clear and, on the other, it can be put in formal terms by making a density expansion of the density-dependent pair interaction up to linear order in density, see Eq. (10) of

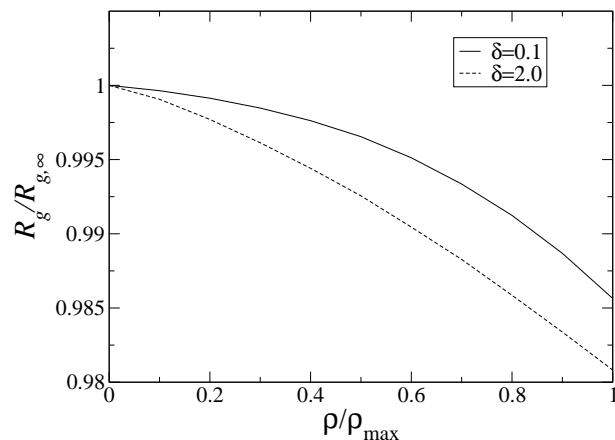


Figure 6. The dependence of the dendrimers' radius of gyration on the solution density for the two types of model macromolecules, as indicated in the legend.

Ref. [17]. Thus, we would then obtain a *weakening* of the correlations and an *increase* of the osmotic compressibility, whereas in Figs. 3 and 4 exactly the opposite is true. In order to obtain the true $g(r)$ at $\rho = \rho_{\max}$ for the $\delta = 0.1$ -dendrimers, a renormalised effective pair potential $\tilde{V}_{\text{eff}}^{(2)}(r; \delta, \rho)$ can be employed that is more strongly repulsive than the original one, $V_{\text{eff}}^{(2)}(r; \delta)$; as a matter of fact, we were able to reproduce $g(r)$ at ρ_{\max} by using $\tilde{V}_{\text{eff}}^{(2)}(r; \delta = 0.1, \rho_{\max}) \cong 1.2 V_{\text{eff}}^{(2)}(r; \delta = 0.1)$. A similar effect has been observed for polymer chains [17], for which the density-dependent, renormalised pair potential necessary to reproduce $g(r)$ at high concentrations was found to be more repulsive than the one that holds at $\rho = 0$, whereas, at the same time, the correction arising from triplet forces alone goes in the opposite direction of weakening the pair repulsions.

The above considerations point to the fact that the deviations between $g(r)$ and $g_{\text{eff}}(r)$ are a genuinely many-body effect that arises from the high concentration of the solution per se and cannot be attributed to three-body forces alone. In particular, the presence of many dendrimers surrounding a given one in the concentrated solution, gives rise to a deformation of the dendrimer itself. To corroborate this statement, we have measured the concentration-dependent monomer density profiles $\xi(u)$ around the dendrimers' centre of mass, given by Eq. (11). Results are shown in Fig. 5(a) for the case $\delta = 0.1$ and in Fig. 5(b) for the case $\delta = 2.0$. It can be seen that as a result of the crowding of the dendrimers at the highest concentration, the monomer profiles become slightly shorter in range and they grow in height; in other words, the dendrimers *shrink* as a result of the increased overall concentration, as can be also witnessed by the reduction of their radius of gyration shown in Fig. 6. The molecules that effectively interact are *stiffer* at higher densities than at lower ones; their internal monomer concentration grows with ρ and as a result of this deformation, the interaction between two dendrimers becomes more repulsive than at zero density.

The above claim is supported by the fact that the effect of the concentration on the pair interaction is much more pronounced for the dendrimers with the short

thread length than for those with the longer one. Although the monomer profiles for *both* dendrimer kinds grow with ρ , the internal monomer concentration for the stiffer dendrimers is much higher than the one for the softer ones. A concentration-induced increase of $\xi(u)$ has a much stronger effect for the effective interaction of the stiff dendrimers than for the soft ones, since it occurs at a scale of $\sigma^3\xi(u) \sim 0.4$ for the former but at a scale of $\sigma^3\xi(u) \sim 0.1$ for the latter, see Fig. 5. The monomer beads are modeled here as hard spheres. The change in the free energy of a hard-sphere fluid upon an increase of the local density is highly nonlinear and grows rapidly with increasing packing fraction, hence the effect is much more pronounced for the case $\delta = 0.1$ than for the case $\delta = 2.0$.

Another way of expressing the vast discrepancy in the monomer crowding of the two systems is to look at the monomer packing fraction η_m . As there are ν monomers per dendrimer, this quantity is given by the expression

$$\eta_m = \frac{\pi}{6}\nu\rho\tau^3\left(\frac{\sigma}{\tau}\right)^3. \quad (17)$$

For both types of dendrimers, $\nu = 62$ and $\rho_{\max}\tau^3 = 0.605$. Yet, the ratio σ/τ has the value 0.188 for $\delta = 0.1$ and 0.101 for $\delta = 2.0$, see the last column of Table 1. Accordingly, at $\rho = \rho_{\max}$ we obtain $\eta_m = 0.13$ for $\delta = 0.1$ but $\eta_m = 0.02$ for $\delta = 2.0$. The soft dendrimers have a much lower monomer packing fraction at ρ_* than the stiffer ones, a result that can be traced to the fact that their radius of gyration is larger.¶ Thus, we conclude that the density-dependence of the pair interaction can be traced back to the shrinking of the dendrimers, a phenomenon that leads to increased crowding of the monomers in their interior.

4. Total scattering intensities and the factorisation approximation

In this section we turn our attention to a different question, which is however related to the issues discussed above, namely to the interpretation of scattering data from concentrated dendrimer solutions. As a first step, we consider the form factor $F(q)$, defined by Eq. (10). Clearly, $F(q)$ expresses the *intramolecular* correlations between the monomers belonging to a certain dendrimer. When scattering from an infinitely dilute solution, $F(q)$ offers the only contribution to the coherent scattering density. Since all the information about the monomer correlations is encoded in $F(q)$, great experimental effort is devoted to the determination of this quantity. At low values of q , $qR_{g,\infty}$, the form factor delivers information about the overall size of the molecule whereas at higher values of the scattering wavevector, $q \sim 1/a$, where a is the monomer length, information about the monomer correlations and the fractal dimension of the object is hidden [1, 33, 35].

Although $F(q)$ is experimentally measured at the limit $\rho \rightarrow 0$, the same quantity can be defined at any density. At arbitrary concentrations, $F(q)$ will in general

¶ This is characteristic for non-compact objects: for polymer chains, e.g., one obtains $\eta_m \sim R_g^{-4/3}$ at the overlap concentration [1].

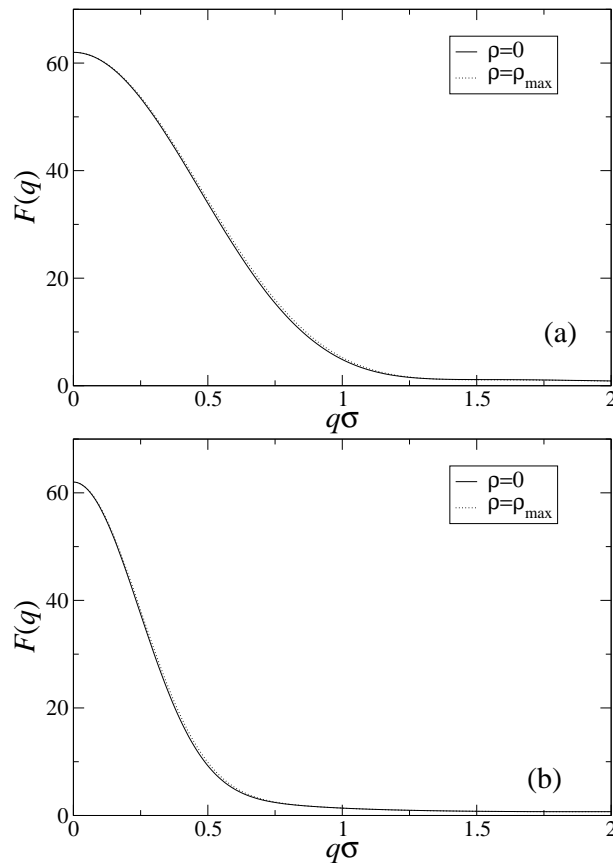


Figure 7. The form factors measured in the monomer-resolved simulations for one isolated dendrimer molecule ($\rho = 0$, solid line) and at the highest density ($\rho = \rho_{\max}$, dotted line). The model dendrimers have maximum thread length (a) $\delta = 0.1$ and (b) $\delta = 2.0$.

change with respect to its form at infinite dilution, due to possible deformations of the macromolecules. In Fig. 7 we show the form factors for the two model dendrimers at the lowest and at the highest simulate densities. It can be seen there that there is only a small change in both cases, which takes the form of a slight extension of $F(q)$ to higher q -values as the concentration increases. This is consistent with the shrinkage of the dendrimers and the corresponding decrease of the gyration radius. Indeed, in the Guinier regime, $qR_g < 1$, the form factor has a parabolic profile, $F(q) \cong N[1 - (qR_g)^2/3]$, and a reduction of R_g manifests itself as a swelling in q -space and vice versa [36].

Let us now turn our attention to the total coherent scattering intensity from all monomers, $I(q)$, given by Eq. (13). It is clear from its definition that $I(q)$ can also be measured in the monomer-resolved simulation and this has been done for both dendrimer species, characterised by the maximum thread extensions $\delta = 0.1$ and $\delta = 2.0$. In attempting to model complex polymeric entities as soft colloids, it is a common procedure to separate the intramolecular from the intermolecular correlations and to write down approximations for the quantity $I(q)$ in which the two types of correlations appear in a factorised fashion. Here we are going to put this approach into a test and

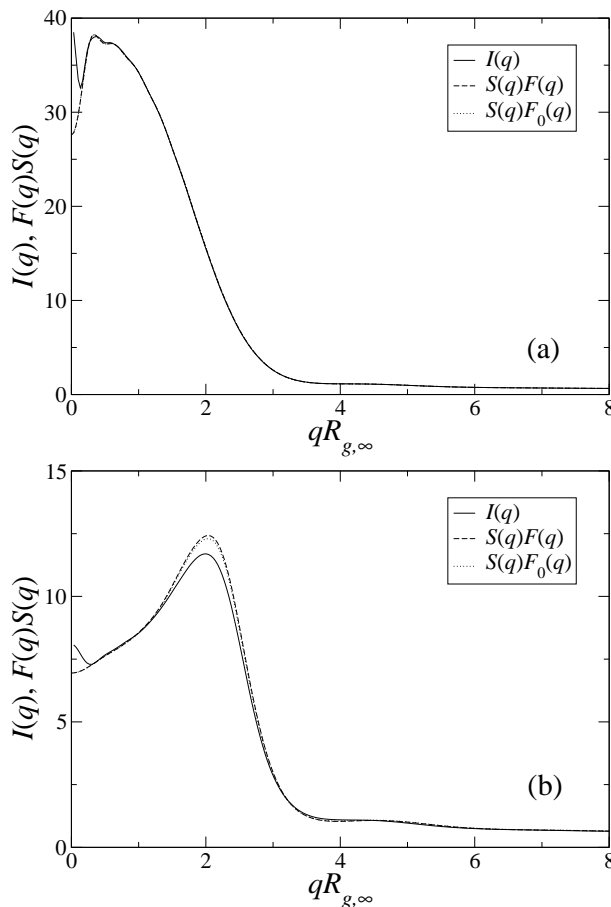


Figure 8. The total coherent scattering intensity $I(q)$ [Eq. (13)] from concentrated $\delta = 0.1$ -dendrimer solutions, compared with the result from the factorisation approximation, Eq. (22), at different overall concentrations ρ . (a) $\rho = 0.1\rho_{\max}$ and (b) $\rho = 0.5\rho_{\max}$. Results using both the form factor $F(q)$ at the given density and its counterpart at infinite dilution, $F_0(q)$ are shown for the factorisation approximation.

figure out the limits of its validity as far as dendritic molecules are concerned. A similar test has been carried out by Krakowiak *et al.* [37] who compared results from the PRISM model for polymers with simulations and with the factorisation ansatz.

As a first approximate step, one assumes that the intramolecular conformations and centre-of-mass correlations decouple from each other. Correspondingly, Eq. (13) takes the approximate form:

$$I(q) \cong \frac{1}{N\nu} \sum_{i=1}^N \sum_{j=1}^N \sum_{\alpha=1}^{\nu} \sum_{\beta=1}^{\nu} \langle \exp[-i\mathbf{q} \cdot (\mathbf{r}_i - \mathbf{r}_j)] \rangle \langle \exp[-i\mathbf{q} \cdot (\mathbf{u}_{\alpha}^i - \mathbf{u}_{\beta}^j)] \rangle. \quad (18)$$

The approximation inherent in Eq. (18) above is a reasonable one for dendrimers. Indeed, as it has been shown in Ref. [38], the monomer degrees of freedom are correlated at length scales $\sim \sigma$, whereas for the overall densities ρ considered here, the centers of mass are correlated at lengths at least $\sim R_g$ and the two are well-separated from each other. Hence, at the wavevector-scale $q_{\text{CM}} \sim 1/R_g$ at which the centre-of-mass

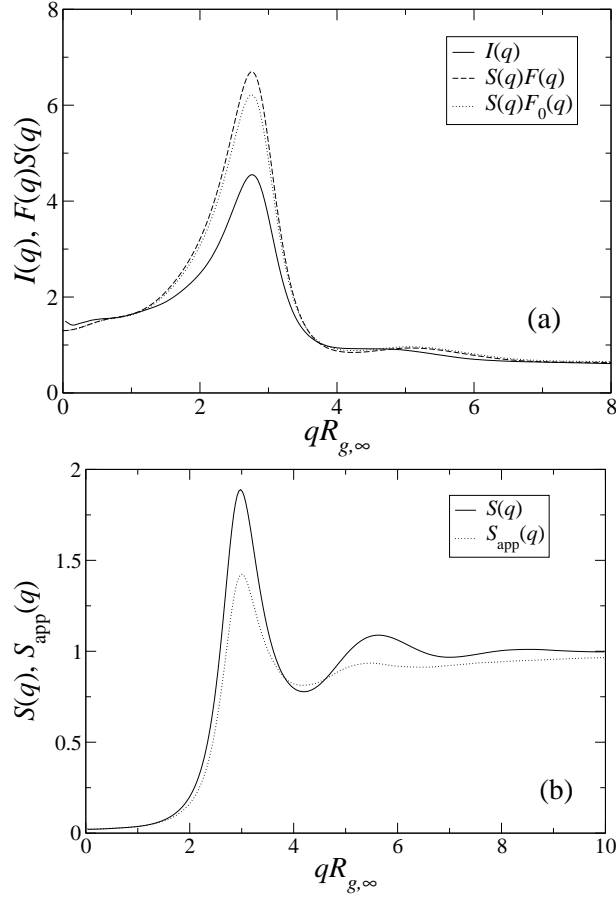


Figure 9. (a) Same as Figs. 8(a) and (b) but for $\rho = \rho_{\max}$. (b) The true structure factor $S(q)$ between the centres of mass at $\rho = \rho_{\max}$, as obtained from the monomer-resolved simulations, compared with the apparent structure factor $S_{\text{app}}(q) = I(q)/F_0(q)$.

$S(q)$ shows structure, the dendrimers still appear as compact objects and the internal fluctuations can be decoupled from the intermolecular ones. The second approximation is now the following. Suppose that we are at sufficiently low densities, so that close approaches between the centres of mass of the dendrimers are very rare and they carry therefore a negligible statistical weight. Then, since monomers belonging to different dendrimers stay far apart, it is reasonable to assume that the deviations from their respective centres of mass are uncorrelated. In this case, one can approximately write:

$$\begin{aligned} \frac{1}{\nu} \sum_{\alpha=1}^{\nu} \sum_{\beta=1}^{\nu} \langle \exp [-i\mathbf{q} \cdot (\mathbf{u}_{\alpha}^i - \mathbf{u}_{\beta}^j)] \rangle &\cong \frac{1}{\nu} \sum_{\alpha=1}^{\nu} \sum_{\beta=1}^{\nu} \langle \exp (-i\mathbf{q} \cdot \mathbf{u}_{\alpha}^i) \rangle \langle \exp (i\mathbf{q} \cdot \mathbf{u}_{\beta}^j) \rangle \\ &= \frac{1}{\nu} \langle \hat{\xi}_{\mathbf{q}} \rangle \langle \hat{\xi}_{-\mathbf{q}} \rangle, \end{aligned} \quad (19)$$

where $\xi_{\mathbf{q}}$ is the Fourier transform of the monomer density operator $\hat{\xi}(\mathbf{u})$ around the

centre of mass of an arbitrary dendrimer:⁺

$$\hat{\xi}(\mathbf{u}) = \sum_{\alpha=1}^{\nu} \delta(\mathbf{u} - \mathbf{u}_{\alpha}^i). \quad (20)$$

Clearly, the right hand side of Eq. (19) has no dependence on the dendrimer index. At the same time, it has been shown in Ref. [38] that the product $\nu^{-1}\langle\hat{\xi}_{\mathbf{q}}\rangle\langle\hat{\xi}_{-\mathbf{q}}\rangle$ is an excellent approximation for the form factor $F(q)$ of the dendrimers, deviations from the exact expression in Eq. (10), $F(q) = \nu^{-1}\langle\hat{\xi}_{\mathbf{q}}\hat{\xi}_{-\mathbf{q}}\rangle$, appearing only at high q -values that are unreachable in a typical SANS experiment. The approximation inherent in Eq. (19) has been derived for monomers belonging to different dendrimers ($i \neq j$) and now, in view of the results of Ref. [38], it can be also applied to the case $i = j$. Putting everything together, we obtain

$$\frac{1}{\nu} \sum_{\alpha=1}^{\nu} \sum_{\beta=1}^{\nu} \langle \exp[-i\mathbf{q} \cdot (\mathbf{u}_{\alpha}^i - \mathbf{u}_{\beta}^j)] \rangle \cong F(q). \quad (21)$$

Eqs. (18) and (21) now yield the oft-employed *factorisation approximation*:

$$I(q) \cong S(q)F(q), \quad (22)$$

whose validity will be tested in what follows.

The assumptions that went into the derivation of Eq. (22) above become exact when the particles from which one scatters are rigid colloids [39], in which case individual scattering centres are devoid of a fluctuating nature. In this context, it is important to note that there is an analog of the factorisation approximation that is applied in the theory of concentrated polymer solutions and carries the name ‘‘rigid particle assumption’’ [37, 40]. Here, one starts from Eq. (18) and assumes that monomer-monomer correlations between monomers belonging to different polymers are identical to the intramolecular correlations in any chain [37]. Under this assumption, the second factor on the right-hand-side of Eq. (18) above takes the form:

$$\frac{1}{\nu} \sum_{\alpha=1}^{\nu} \sum_{\beta=1}^{\nu} \langle \exp[-i\mathbf{q} \cdot (\mathbf{u}_{\alpha}^i - \mathbf{u}_{\beta}^j)] \rangle \cong \frac{1}{\nu} \sum_{\alpha=1}^{\nu} \sum_{\beta=1}^{\nu} \langle \exp[-i\mathbf{q} \cdot (\mathbf{u}_{\alpha}^i - \mathbf{u}_{\beta}^i)] \rangle = F(q), \quad (23)$$

and, in conjunction with Eq. (18), the factorisation approximation of Eq. (22) follows once again. Krakoviak *et al.* tested the validity of Eq. (22) for polymer solutions, finding that it breaks down for high polymer densities.

We have put the validity of Eq. (22) into a strong test by comparing the directly measured total coherent scattering intensity $I(q)$ with the product $F(q)S(q)$, where for the latter quantity both factors are the ones measured in the same simulation. Results are shown in Figs. 8 and 9(a) for the $\delta = 0.1$ -dendrimers as well as in Figs. 10 and 11(a) for the $\delta = 2.0$ -dendrimers. It can be seen that the factorisation approximation is valid at the lowest density shown ($\rho = 0.1\rho_{\max}$) but that its quality becomes poorer as the concentration of the solution increases. A dramatic breakdown can be seen in Fig.

⁺ The quantity $\xi(\mathbf{u})$ defined in Eq. (11) is simply the expectation value of the operator $\hat{\xi}(\mathbf{u})$.

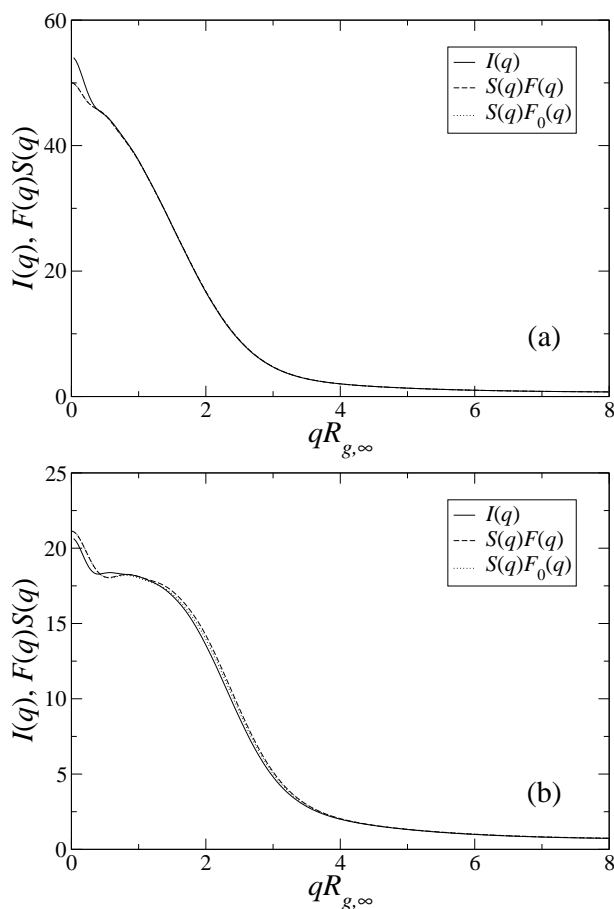


Figure 10. Same as Fig. 8 but for $\delta = 2.0$ -dendrimers.

9(a) for the more compact dendrimers, whereas the breakdown is also clear (but less spectacular) for the more open dendrimers, Fig. 11(a).

We can now trace back to the physical origins of the breakdown of the factorisation approximation, Eq. (22). There is first of all a weak breakdown of the first assumption, Eq. (18), in which the centre-of-mass coordinates were decoupled from the fluctuating monomers. Indeed, were this approximation to be true, then the form factor $F(q)$ would remain unchanged at all concentrations. This is however not the case, as the results in Fig. 7 demonstrate: the dendrimers shrink as ρ grows. Yet, the difference between the infinite-dilution form factor, $F_0(q)$ and its counterpart at finite density, $F(q)$, is not sufficient to account for the failure of the factorisation approximation. As can be seen in Figs. 8(b), 9(a), 10(b) and 10(a), the product $S(q)F(q)$ is in even *worse* agreement with $I(q)$ than the product $S(q)F_0(q)$. The reason for the breakdown of Eq. (22) lies in the assumption inherent in deriving the approximation of Eq. (21), namely that fluctuations between monomers belonging to different dendrimers are uncorrelated. At sufficiently low densities ρ , this is a reasonable assumption. However, in approaching the overlap density ρ_* , it does not hold any more. As monomers from different dendrimers begin to crowd with one another, their coordinates with respect to their centers of mass become

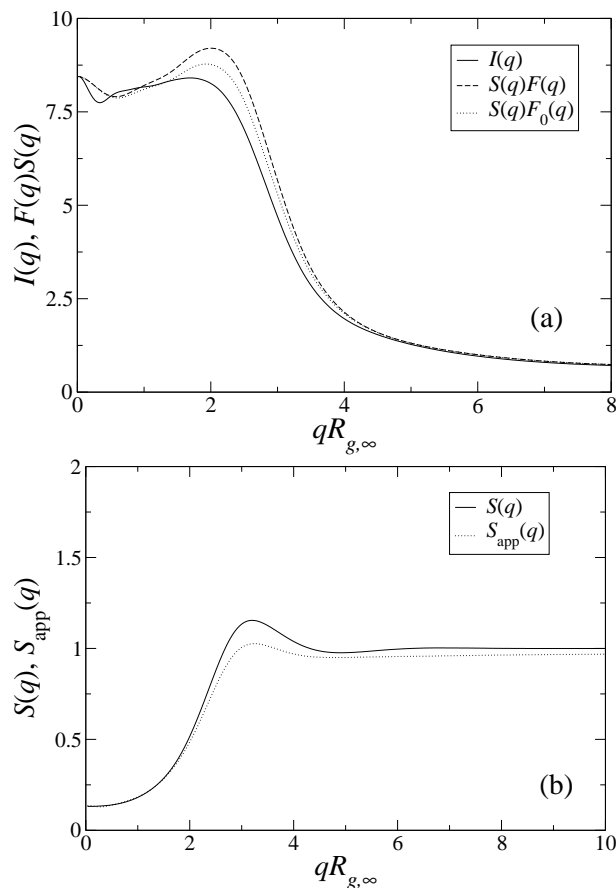


Figure 11. Same as Fig. 9 but for $\delta = 2.0$ -dendrimers.

more and more strongly correlated and Eq. (21) loses its validity. In this respect, it is not surprising that the breakdown of Eq. (22) is more dramatic for the $\delta = 0.1$ -dendrimers than for the $\delta = 2.0$ -ones. In the former case, the monomer packing fraction is higher and the corresponding correlations between monomers belonging to different molecules stronger than in the latter. To put it in more pictorial terms: at the overlap concentration it is not any more possible to tell to which dendrimer a monomer belongs, see Fig. 2. A clear separation between intra- and inter-dendrimer fluctuations is not any more possible.

We finally discuss the consequences of the above findings for the interpretation of scattering data obtained from concentrated dendrimer solutions. The validity of Eq. (22) is often taken for granted: the form factor $F(q)$ is measured in a SANS- or SAXS experiment at low concentrations and extrapolated to infinite dilution to obtain the quantity $F_0(q)$. Thereafter, the measured coherent scattering intensity at any concentration, $I(q)$ is divided through $F_0(q)$, the result being interpreted as the structure factor of the system. In order to differentiate it from $S(q)$, we emphasise here that this is only an *apparent* structure factor $S_{app}(q)$, given by

$$S_{app}(q) = \frac{I(q)}{F_0(q)}. \quad (24)$$

In Figs. 9(b) and 11(b) we compare the apparent structure factors for the two dendrimer species at the highest simulated density with the true ones. It can be seen that the process of applying Eq. (24) has the effect of producing apparent structure factors that are everywhere lower than the true ones and they even fail to reach the asymptotic value unity at the range considered.

Such structure factors from concentrated dendrimer solutions have been published in Refs. [41] and [42], in which they have been correctly termed ‘apparent’. It is important here to point out that apparent structure factors can lead to false conclusions regarding the validity of the pair potential approximation in mesoscopic theories of dendrimer solutions. Indeed, as we have explicitly shown in this work, many-body effective potentials play only a minor role in concentrated dendrimer solutions, therefore, one can obtain accurate structure factors from theory by working with a density-independent pair potential. If, however, these structure factors were to be compared with the apparent experimental quantities $S_{\text{app}}(q)$, discrepancies of the kind shown in Figs. 9(b) and 11(b) would show up. It would be then possible to argue that these discrepancies are due to the breakdown of the pair potential approximation but, as we have shown here, this conclusion would be unwarranted. The reason for the disagreement between theory and ‘experiment’ would, in this case, lie in the employment of an *erroneous* approximation, Eq. (22), in deriving apparent structure factors from the experimental data. It is worth noting that Krakoviak *et al.* [37] reached similar conclusions for the case of polymer solutions, although they did not formally introduce an apparent structure factor into their considerations.

5. Summary and concluding remarks

We have carried out extensive, monomer-resolved and effective simulations of model dendrimers in order to calculate correlation functions between the centres of mass of the macromolecules and the individual monomers themselves. By comparing the real-space correlation functions obtained by the two simulation approaches, we found that many-body effective potentials play a minor role up to the overlap density and they can be altogether ignored for open dendrimers with long bond lengths. Our finding for the scattering intensity, on the other hand, is that the factorisation approximation of this quantity into a form- and a structure factor loses its validity as one approaches the overlap concentration. Structure factors that are obtained from experimental data by dividing the scattering intensity through the form factor can be seriously in error.

It appears, therefore, that the extraction of an accurate structure factor from concentrated dendrimer solutions is extremely difficult as one approaches the overlap concentration. We anticipate that this result is also valid for other ‘polymeric colloids’ such as star-shaped polymers and brushes. One strategy to circumvent this inherent difficulty is to use the labeling technique, in which a small, inner part of the molecule is protonated and the rest is deuterated in such a way that the contrast between the outermost part of the molecule and the solvent vanishes. In this way, only the innermost

part of the molecule will have contrast with the solvent and scatter coherently. Thus, one can reach concentrations for the whole system that exceed ρ_* , whereas the labeled parts are still nonoverlapping. Such a technique was successfully applied, e.g., to star polymers [12].

Acknowledgments

This work has been supported by the Deutsche Forschungsgemeinschaft (DFG).

References

- [1] Likos C N 2001 *Phys. Rep.* **348** 267
- [2] Dijkstra M, Brader J M and Evans R 1999 *J. Phys.: Condens. Matter* **11** 10079
- [3] Dijkstra M, van Roij R and Evans R 1998 *Phys. Rev. Lett.* **81** 2268; 1999 *ibid.* **82** 117
- [4] Dijkstra M, van Roij R and Evans R 1999 *Phys. Rev. E* **59** 5744
- [5] Hansen J P and Löwen H 2000 *Ann. Rev. Phys. Chem.* **51** 209
- [6] Louis A A 2002 *J. Phys.: Condens. Matter* **14** 9187
- [7] Stillinger F H, Sakai H and Torquato S 2003 *J. Chem. Phys.* **117** 288
- [8] Sakai H, Stillinger F H and Torquato S 2003 *J. Chem. Phys.* **117** 297
- [9] Dijkstra M, van Roij R and Evans R 2000 *J. Chem. Phys.* **113** 4799
- [10] Axilrod B M and Teller E 1943 *J. Chem. Phys.* **11** 229
- [11] Tau M, Reatto L, Magli R, Egelstaff P A and Barrochi F 1989 *J. Phys.: Condens. Matter* **1** 7131
- [12] Likos C N, Löwen H, Watzlawek M, Abbas B, Jucknischke O, Allgaier J and Richter D 1998 *Phys. Rev. Lett.* **80** 4450
- [13] Jusufi A, Dzubiella J, Likos C N, von Ferber C and Löwen H 2001 *J. Phys.: Condens. Matter* **13** 6177
- [14] Krüger B, Schäfer L and Baumgärtner A 1989 *J. Phys. (Paris)* **50** 3191
- [15] Louis A A, Bolhuis P G, Hansen J P and Meijer E J 2000 *Phys. Rev. Lett.* **85** 2522
- [16] Louis A A, Bolhuis P G and Hansen J P 2000 *Phys. Rev. E* **62** 7961
- [17] Bolhuis P G, Louis A A and Hansen J P 2001 *Phys. Rev. E* **64** 021801
- [18] Bolhuis P G, Louis A A and Hansen J P 2001 *J. Chem. Phys.* **114** 4296
- [19] Löwen H and Allahyarov E 1998 *J. Phys.: Condens. Matter* **10** 4147
- [20] Brunner M, Dobnikar J, von Grünberg H H and Bechinger C 2004 *Phys. Rev. Lett.* **92** 078301
- [21] Dobnikar J, Brunner M, von Grünberg H H and Bechinger C 2004 *Phys. Rev. E* **69** 031402
- [22] von Ferber C, Jusufi A, Likos C N, Löwen H and Watzlawek M 2000 *Eur. Phys. J. E* **2** 311
- [23] Ballauff M and Likos C N 2004 *Angewandte Chemie Intl. English Ed.* **43** 2998
- [24] Likos C N, Schmidt M, Löwen H, Ballauff M, Pötschke D and Lindner P 2001 *Macromolecules* **34** 2914
- [25] Likos C N, Rosenfeldt S, Dingenouts N, Ballauff M, Lindner P, Werner N and Vögtle F 2002 *J. Chem. Phys.* **117** 1869
- [26] Götze I O, Harreis H M and Likos C N 2004 *J. Chem. Phys.* **120** 7761
- [27] Sheng Y J, Jiang S and Tsao H K 2002 *Macromolecules* **35** 7865
- [28] Götze I O and Likos C N 2003 *Macromolecules* **36** 8189
- [29] Hansen J P and McDonald I R 1986 *Theory of Simple Liquids* 2nd ed (London: Academic)
- [30] Pötschke D, Ballauff M, Lindner P, Fischer M and Vögtle F 1999 *Macromolecules* **32** 4079
- [31] Pötschke D, Ballauff M, Lindner P, Fischer M and Vögtle F 2000 *Macromol. Chem. Phys.* **201** 330
- [32] Rosenfeldt S, Dingenouts N, Ballauff M, Lindner P, Likos C N, Werner N and Vögtle F 2002 *Macromol. Chem. Phys.* **203** 1995

- [33] Higgins J S and Benoît H C 1994 *Polymers and Neutron Scattering* (Oxford: Clarendon)
- [34] It is intriguing, in this respect, that the three-body forces are also attractive for charged colloids, see Refs. [20] and [21]. However, in the latter case the many-body forces arise through nonlinear counterion screening and the corresponding rearrangements of the counterion clouds, hence a direct analogy with the case at hand cannot be made.
- [35] For an illuminating review on experimental aspects of scattering from polymeric systems see the article: Grest G S, Fetters L J, Huang J S and Richter D 1996 *Adv. Chem. Phys.* **XCIV** 67
- [36] Likos C N, Löwen H, Poppe A, Willner L, Roovers J, Cubitt B and Richter D 1998 *Phys. Rev. E* **58** 6299
- [37] Krakoviak V, Hansen J P and Louis A A 2002 *Europhys. Lett.* **58** 53
- [38] Harreis H M, Likos C N and Ballauff M 2003 *J. Chem. Phys.* **118** 1979
- [39] Klein R and D' Aguanno B 1996 in *Light Scattering: Principles and Development*, edited by W Brown (Oxford: Clarendon)
- [40] Pagonabarraga I and Cates M E 2001 *Europhys. Lett.* **55** 348
- [41] Topp A, Bauer B J, Prosa T J, Scherrenberg R and Amis E J 1999 *Macromolecules* **32** 8923
- [42] Ramzi A, Scherrenberg R, Brackman J, Joosten J and Mortensen K 1998 *Macromolecules* **31** 1621